

# Identifying charge and pairing density waves in X-ray scattering experiments

David Dentelski<sup>1,2</sup> and Emanuele G. Dalla Torre<sup>1,2</sup>

<sup>1</sup>*Department of Physics, Bar-Ilan University, 52900, Ramat Gan Israel*

<sup>2</sup>*Center for Quantum Entanglement Science and Technology, Bar-Ilan University, 52900, Ramat Gan Israel*

Competing density waves play an important role in the mystery of high-temperature superconductors. In spite of the large amount of experimental evidence, the fundamental question of whether these modulations represent charge or pairing density waves (CDWs or PDWs) is still debated. Here we present a method to answer this question using two-dimensional X-ray scattering maps. Starting from a minimal model of the superconducting state of cuprates, we identify the distinctive signatures of incipient CDWs and PDWs. The generality of our approach is confirmed by both a heuristic model of the Fermi surface and a self-consistent solution of an extended Hubbard model with attractive interaction. By considering the available experimental data, we claim that the spatial modulations in cuprates have a predominant PDW character. Our work paves the way for using X-ray to identify competing and intertwined orders in superconducting materials.

*Introduction* - Strongly correlated materials often exhibit competing phases with distinct charge and spin orders. A famous example are cooper-oxide high-temperature superconductors, or cuprates, whose rich phase diagram poses many theoretical challenges. Since the discovery of unidirectional spin density waves in LSCO [1], it has become increasingly accepted that in cuprates superconductivity is intertwined with other orders [2–6]. In particular, in 2002, scanning tunneling experiments found incommensurate density waves on the surface of BSCCO [7–10]. Ten years later, elastic X-ray scattering experiments detected a similar incommensurate order in the bulk of YBCO [11]. The same order was later found in a large number of cuprates, demonstrating that this effect is ubiquitous [12–29].

In spite of the large number of experimental studies, the physical interpretation of these periodic modulations is still debated. A common approach, also based on earlier theoretical predictions [30, 31], claims that these modulations are due to a charge density wave (CDW) order that competes with superconductivity. While this approach is widely accepted in the literature, it is inconsistent with some experimental details. In particular, angle-resolved photoemission spectroscopy (ARPES) shows that these density waves are associated with a spectral gap that closes from below the Fermi energy [32], while CDWs' gaps are expected to close from above. Accordingly, it was argued that the competing order is rather a pair density wave (PDW) [33, 34], or a CDW/PDW mixed order [35–38]. This claim is also supported by recent scanning measurements in the halos of magnetic vortices [39] and with superconducting tips [40] (see Ref. [41] for a recent review).

Here we address the question of how to distinguish between CDW and PDW modulations in available X-ray scattering experiments. Our approach departs from earlier studies, which were based on controversial descriptions of the normal state of cuprates, such as Fermi liquids [42, 43], Fermi gases with strong antiferromagnetic fluctuations [44], and Fermi arcs with hot spots

[35–38, 45, 46]. Instead, we base our analysis on the undisputed description of the superconducting state of cuprates in terms of a Bardeen-Cooper-Schrieffer (BCS) Hamiltonian with a d-wave gap. In this phase, superconductivity suppresses competing orders, justifying a weak-coupling approach where the density waves are induced by weak pinning centers [47, 48]. This approach allows us to develop a rigorous method to distinguish between incipient CDW and PDW fluctuations, which become long-ranged at high magnetic fields. The validity of this approach is confirmed by the solution of an extended Hubbard model with attractive interactions in the presence of local impurities, which enables us to study the interplay between CDWs and PDWs.

*Weak coupling approach* – In X-ray experiments, the intensity of scattered light at a wavevector  $q$  is proportional to the intensity of the density modulations at the same wavevector,  $n_{\mathbf{q}}$  [49]. Weak CDWs and PDWs can be modeled by a homogeneous state perturbed by a local pinning center (impurity). In this approximation,  $\langle n_{\mathbf{q}} \rangle = \lim_{\Omega \rightarrow i0^+} \chi(\mathbf{q}, \Omega)$ , where  $\chi$  is the density response to the impurity. In the case of a superconducting state described by the BCS model at zero temperature (see, for example, Ref.[50]), one finds

$$\chi(\mathbf{q}, \Omega) = \int d\omega \int d^d k \text{Tr} [G_0(\mathbf{k}, \omega) V_{\mathbf{k}} G_0(\mathbf{k} + \mathbf{q}, \omega + \Omega) \sigma^z]. \quad (1)$$

Here  $V$  models a static (time independent) and local ( $q$  independent) impurity and  $\sigma^z$  is a Pauli matrix. The Green's function  $G_0$  is given by

$$G_0^{-1}(\mathbf{k}, \omega) = \begin{pmatrix} -\omega + \varepsilon_{\mathbf{k}} - \mu & \Delta_{\mathbf{k}} \\ \Delta_{\mathbf{k}}^* & -\omega - \varepsilon_{\mathbf{k}} + \mu \end{pmatrix}, \quad (2)$$

where  $\Delta_{\mathbf{k}} = \frac{\Delta_0}{2}(\cos(k_x) - \cos(k_y))$  is the pairing gap,  $\varepsilon_{\mathbf{k}}$  is the band structure of the material, and  $\mu$  the chemical potential [51].

Let us first consider weak CDW modulations, by introducing a local charge impurity,  $V_{\mathbf{k}} = V_0 \sigma^z$ . For this

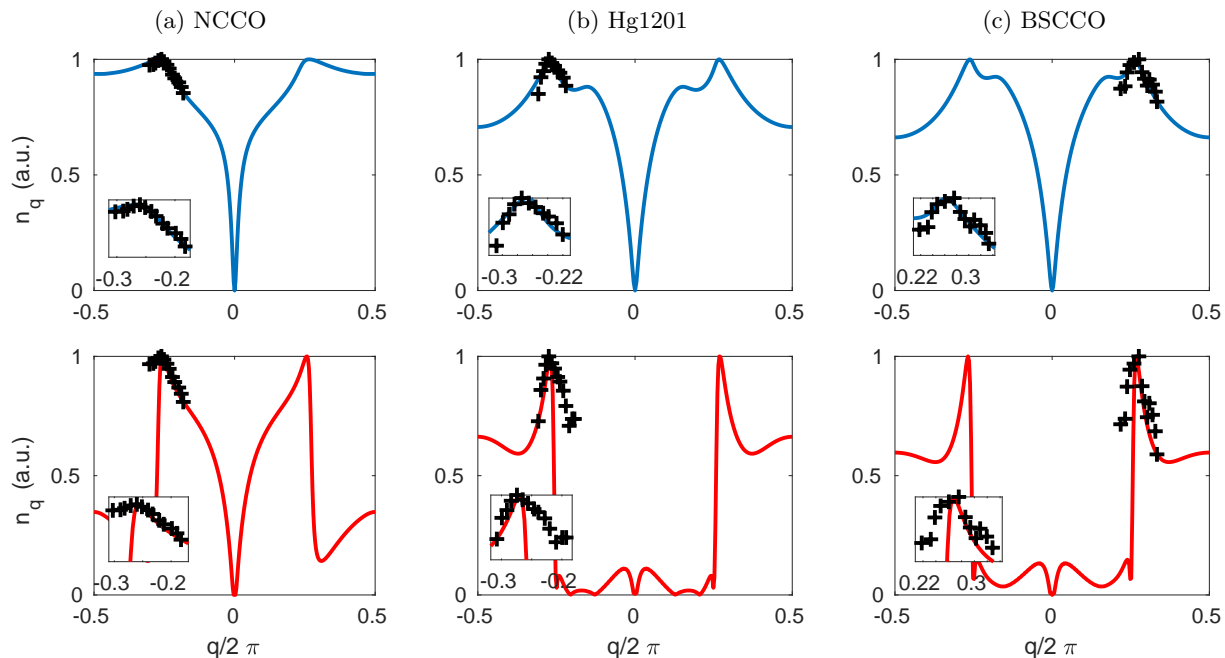


FIG. 1. Density fluctuations induced by charge (upper panel) and pairing (lower panel) pinning centers, for three superconducting cuprates. The experiments (crosses) are reproduced from (a) electron doped NCCO,  $x = -0.14$  [27]; (b) underdoped Hg1201,  $x = 0.09$  [19]; (c) underdoped BSCCO,  $x = 0.12$  [15]. The theoretical curves shown in the upper (lower) panel were obtained from Eq. (3) [Eq. (4)] with  $\Delta_0/t = 0.1$  ( $\Delta_0/t = 0.3$ ) and (a)  $t'/t = -0.22$  ( $-0.4$ ), (b)  $t'/t = -0.7$  ( $-0.7$ ), (c)  $t'/t = -0.7$  ( $-0.7$ ).

impurity, the integral over  $\omega$  in Eq. (1) delivers

$$n_{\mathbf{q}} = 2\pi V_0 \int d^2k \left[ \frac{E_{\mathbf{k}}^2 + \varepsilon_{\mathbf{k}}\varepsilon_{\mathbf{k}+\mathbf{q}} - \Delta_{\mathbf{k}}\Delta_{\mathbf{k}+\mathbf{q}}}{E_{\mathbf{k}}(E_{\mathbf{k}+\mathbf{q}}^2 - E_{\mathbf{k}}^2)} + \frac{E_{\mathbf{k}+\mathbf{q}}^2 + \varepsilon_{\mathbf{k}}\varepsilon_{\mathbf{k}+\mathbf{q}} - \Delta_{\mathbf{k}}\Delta_{\mathbf{k}+\mathbf{q}}}{E_{\mathbf{k}+\mathbf{q}}(E_{\mathbf{k}}^2 - E_{\mathbf{k}+\mathbf{q}}^2)} \right], \quad (3)$$

where  $E_{\mathbf{k}} = \sqrt{\varepsilon_{\mathbf{k}}^2 + \Delta_{\mathbf{k}}^2}$ . In the limit of  $\Delta_{\mathbf{k}} \rightarrow 0$ , one has  $E_{\mathbf{k}} = |\varepsilon_{\mathbf{k}}|$  and Eq. (3) recovers the Lindhard response function of free fermions used in Ref. [42].

To describe X-ray scattering experiments of cuprates, we use a minimal tight-binding model,  $\varepsilon_{\mathbf{k}} = -2t[\cos(k_x) + \cos(k_y)] - 4t' \cos(k_x) \cos(k_y)$ , where  $t$  and  $t'$  are nearest neighbor (NN) and next-nearest neighbor (NNN) hoppings. The parameter  $t'$  strongly affects the shape of the Fermi surface: superconducting cuprates are close to half-filling and, for  $t' = 0$ , their Fermi surface has a diamond shape. A negative  $t'$  leads to a Fermi surface with parallel segments (nesting) at the antinodal wavevectors  $\mathbf{k} = (\pm\pi/a, 0)$  and  $(0, \pm\pi/a)$ . As pointed out long ago [52], these parallel segments are prone to induce finite wavevector instabilities, such as CDWs and PDWs. This approach matches the experimentally observed doping dependence of the wavevector [53].

In the upper panel of Fig. 1, we compare Eq. (3) with resonant X-ray scattering of three different cuprates [54]: electron-doped NCCO [27], underdoped BSCCO [15] and

underdoped Hg1201 [19]. In these plots we select  $\mu$  to match the experimental doping  $x$ . The superconducting gap  $\Delta_0$  has a minor influence on these plots and is set to physically relevant values. The fitting parameter  $t'$  is obtained by minimizing the difference between the theoretical curves and the actual experiments. The values of  $t'/t$  obtained by this procedure are consistent with the Fermi surfaces determined by ARPES [55, 56]. For all three materials, we obtain an excellent agreement between the theoretical curves and the experiments: Eq. (3) describes well both the period of the modulation and the width of the peak.

As mentioned above, an alternative explanation for the observed signal are PDW fluctuations. Here, one needs to distinguish between a state in which the pairing averages to zero and has only spatial modulations and a state in which the PDW fluctuations coexist with a constant pairing gap  $\Delta_0$ . The former situation, analogous to the FFLO state [57, 58], can account for some of the experimental features in stripe superconductors (such as LBCO near 1/8 doping [59, 60]). In contrast, we focus here on the latter scenario by considering a pinning center that corresponds to a local modulation of the pairing gap,  $V_{\mathbf{k}} = \Delta_{\mathbf{k}}\sigma^x$  in Eq. (1), where  $\sigma^x$  is a Pauli matrix. By performing the integral over  $\omega$  in Eq. (1), we obtain

$$n_{\mathbf{q}} = 2\pi \int d^2k \Delta_{\mathbf{k}} \frac{\varepsilon_{\mathbf{k}}\Delta_{\mathbf{k}+\mathbf{q}} + \varepsilon_{\mathbf{k}+\mathbf{q}}\Delta_{\mathbf{k}}}{(E_{\mathbf{k}} - E_{\mathbf{k}+\mathbf{q}})E_{\mathbf{k}}E_{\mathbf{k}+\mathbf{q}}}. \quad (4)$$

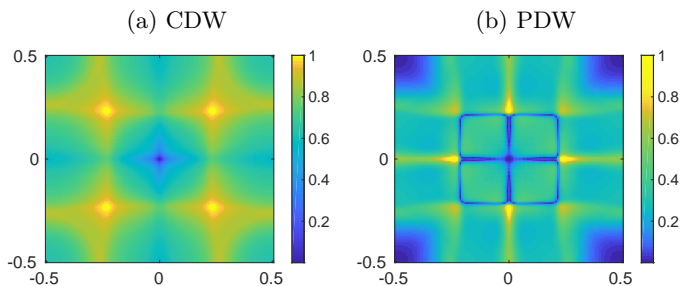


FIG. 2. Two dimensional maps of the density fluctuations  $n_{\mathbf{q}}$  in the weak-coupling approach: (a) CDW, Eq. (3), (b) PDW, Eq. (4). Numerical parameters:  $x = 0.14$ ,  $t'/t = -0.6$ ,  $\Delta_0/t = 0.1$  for CDW and  $\Delta_0/t = 0.3$  for PDW.

The corresponding plots are shown in the lower panel of Fig. 1. We find that the PDW signal shows pronounced peaks at approximately the same wavevector as the CDW one. The precise shape of the peaks depends on the details of the band structure and cannot be used to identify the type of modulation. As a result, one-dimensional scans of the X-ray scattering are not sufficient to distinguish unequivocally between CDW and PDW fluctuations.

*Identifying CDW and PDW* – To distinguish between these two types of modulations, one needs to inspect the full two dimensional map of  $n_{\mathbf{q}}$ . Two representative theoretical maps are shown in Fig. 2. Although both maps have pronounced peaks at the same wave-vector ( $q \approx \pm 0.25$ ), their two-dimensional structure is very different: The CDW signal has four peaks at  $\mathbf{q} = (\pm q, \pm q)$  and four saddle points at  $\mathbf{q} = (0, \pm q)$  and  $(\pm q, 0)$ . In contrast, the PDW signal has four strong peaks at  $\mathbf{q} = (0, \pm q)$  and  $(\pm q, 0)$  and four weaker peaks at  $\mathbf{q} = (\pm q, \pm q)$ . We claim that the ratio between the intensity of the signal at these two wavevectors can be used to identify the type of modulation. For the parameters used in Fig. 2, we find

$$R \equiv \frac{n_{(q,0)}}{n_{(q,q)}} \approx \begin{cases} 0.8 & \text{for CDW,} \\ 1.4 & \text{for PDW.} \end{cases} \quad (5)$$

This result is very robust: Although the precise value of  $R$  depends on the microscopic parameters of the model, we find generically that  $R < 1$  for CDWs and  $R > 1$  for PDWs.

To understand this result, let us consider the simplified version of the Fermi surface of cuprates shown in Fig. 3(a). Due to the denominator in Eqs. (3), CDWs are mostly affected by  $\mathbf{k}$  vectors such that  $\varepsilon_{\mathbf{k}} \approx \varepsilon_{\mathbf{k}+\mathbf{q}} \approx 0$ . Hence, this signal is naturally enhanced at nesting vectors  $\mathbf{q}$  that connect parallel segments of the Fermi surface. In the Fermi surface of Fig. 3, the nesting condition is achieved at both  $(q, 0)$  and  $(q, q)$ . As shown there, the segments of the Fermi surface contributing to the former (rectangles) are shorter than the segments contributing to the latter (rectangles and ellipses): their total lengths

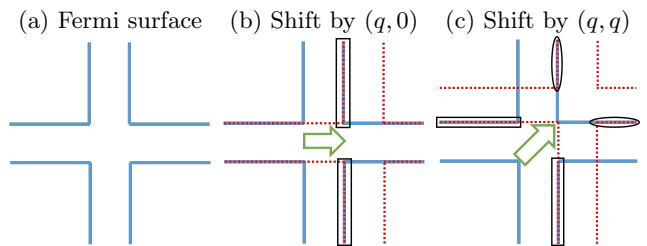


FIG. 3. (a) Simplified model of the Fermi surface of cuprates with well-defined nesting vectors. (b) Overlap between the Fermi surfaces  $\varepsilon_{\mathbf{k}} = 0$  and  $\varepsilon_{\mathbf{k}+(q,0)} = 0$ . (c) Overlap between the Fermi surfaces  $\varepsilon_{\mathbf{k}} = 0$  and  $\varepsilon_{\mathbf{k}+(q,q)} = 0$ . The black rectangles and ellipses indicate the segments of the Fermi surface that contribute to  $n_{\mathbf{q}}$  (see text).

equal to, respectively,  $2\pi/a - q$  and  $4\pi/a - 4q$ . Hence, for  $q = 0.25 \times 2\pi/a$ , this model predicts that  $R = 3/4$ , in quantitative agreement with Eq. (5). In the case of the PDW signal, Eq. (4), each segment of the Fermi surface is weighted by the corresponding value of  $\Delta_{\mathbf{k}}$ . This factor strongly favors the wavevector  $(q, 0)$ , which connects antinodes to antinodes, with respect to  $(q, q)$ , which connects antinodes to nodes. Hence, for PDWs  $R > 1$ , as in Eq. (5).

The experimental data strongly supports the PDW scenario: (i) the scattering amplitudes at wavevectors in the vicinity of  $(q, 0)$  show that this is a peak, rather than a saddle point [26], and (ii) the peak at  $(q, q)$  is small [61] or absent [29, 43], indicating that  $R > 1$ . Both observations are consistent with the PDW scenario only.

*Hubbard model* – The weak coupling approach considered above does not take into account the interactions between quasiparticles, which can enhance the CDW and PDW fluctuations and lead to a competition between them. To capture these effects, we now consider a two-dimensional extended Hubbard model with on-site repulsion  $U$  and NN attraction  $V$ . This model shows several competing phases, such as the Mott insulator and the d-wave superconductor, that are generic to cuprates [62–66]. Under the usual mean-field approximation  $n_j = \sum_{\sigma=\pm} \langle c_{j,\sigma}^\dagger c_{j,\sigma} \rangle / 2$ ,  $\Delta_{\hat{e},j} = \sum_{\sigma=\pm} \sigma \langle c_{j,-\sigma} c_{j+\hat{e},\sigma} \rangle / 2$ , the Hamiltonian reads

$$H = -t \sum_{\langle i,j \rangle, \sigma} c_{i,\sigma}^\dagger c_{j,\sigma} - t' \sum_{\langle\langle i,j \rangle\rangle, \sigma} \left( c_{i,\sigma}^\dagger c_{j,\sigma} + \text{H.c.} \right) \quad (6)$$

$$+ U \sum_{j,\sigma} n_j c_{j,\sigma}^\dagger c_{j,\sigma} + V \sum_{\hat{e},j,\sigma} \left( \Delta_{\hat{e},j} c_{j,\sigma}^\dagger c_{j+\hat{e},\sigma} + \text{H.c.} \right)$$

where  $\langle \cdot, \cdot \rangle$  denotes NN,  $\langle\langle \cdot, \cdot \rangle\rangle$  denotes NNN,  $\hat{e}$  connects NN sites, and H.c. stands for Hermitian conjugate. For  $V < 0$  and  $0 < U \lesssim |V|$ , the self-consistent solution of Eq. (6) delivers a superconductor with d-wave order parameter  $\Delta_j = \frac{1}{4}(\Delta_{\hat{x},j} + \Delta_{-\hat{x},j} - \Delta_{\hat{y},j} - \Delta_{-\hat{y},j})$ .

To study the interplay between CDW and PDW we now consider two types of impurities acting as pinning

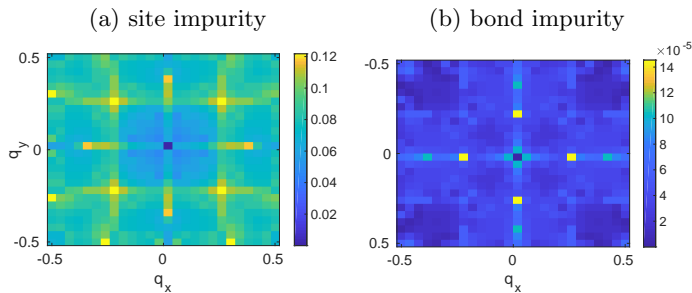


FIG. 4. Two dimensional maps of the density fluctuations  $n_{\mathbf{q}}$  in the Hubbard model with a local modulation of the interaction: (a) on a single site, (b) on a single bond. For clarity, subfigure (b) has been symmetrized by 90 degrees. Numerical parameters:  $x = 0.16$ ,  $t'/t = -0.6$  and  $U/t = -V/t = 0.5$ ,  $\delta U/t = \delta V/t = 0.2$ .

centers: a single site on which  $U \rightarrow U + \delta U$  and a single bond on which  $V \rightarrow V + \delta V$ . Our numerical calculations reveal that both pinning centers lead to periodic modulations in the charge  $n_j$  and in the pairing gap  $\Delta_j$ . We classify these modulations as CDW or PDW depending on which modulation is dominant. This can be achieved by comparing the relative standard deviations  $\delta n$  and  $\delta \Delta$  [67]. For an on-site impurity, we obtain  $\delta n/\delta \Delta \approx 1$ , while for a bond impurity  $\delta n/\delta \Delta \approx 0.007$ . Hence, our model predicts that a site defect leads to a mixed CDW/PDW signal, while a bond defect leads to a dominant PDW signal.

Let us now turn to the Fourier transformed density  $n_{\mathbf{q}}$  shown in Fig. 4. As expected, we find that interactions enhance density wave instabilities and lead to narrower peaks, with longer range correlations. In our calculations, the width of these peaks is limited by the system size ( $L = 26$  unit cells), suggesting that the Hubbard model is consistent with long ranged CDW/PDW modulations. By comparing the two subplots, we observe that the on-site impurity leads to peaks at both wavevectors  $(q, q)$  and  $(q, 0)$ , while the bond impurity leads to pronounced peaks in at the wavevector  $(q, 0)$  only. This is consistent with our proposal to compare the intensities of the two peaks to distinguish between CDW and PDW modulations.

*Discussion* – In this Letter we described a method to distinguish between incipient CDW and PDW fluctuations, based on the analysis of X-ray scattering experiments. When these spatial modulations coexist with an homogeneous superconducting gap  $\Delta_0$ , both oscillations couple directly to any physical observable, such as the charge density and the tunneling density of states. Hence, both CDWs and PDWs can be detected using different experimental technique, including X-ray scattering, scanning tunneling spectroscopy (STS), and scanning Josephson probes. Here we focused on X-ray scattering and showed that one-dimensional cuts are not unambiguous, because they can be adequately fitted by both

types of modulations. In contrast, two-dimensional maps of CDWs and PDWs are very different: the former are peaked at wavevector  $(q, q)$ , while the latter has stronger peaks at  $(q, 0)$ . We supported this claim by a minimal model of the superconducting state of cuprates, as well as a heuristic model of a cross-shaped Fermi surface. By considering an attractive Hubbard model, we demonstrated that our method to identify fluctuations with a dominant CDW or PDW character remains valid in the presence of strong interactions. In particular, we showed that bond-centered impurities induce long ranged PDWs at wavevector  $(q, 0)$ .

Our theoretical model reproduces the main features of X-ray scattering experiments of superconducting NCCO, Hg1201, and BSCCO. Specifically, our theory explains why the experimental signal is peaked at  $(q, 0)$ , rather than at  $(q, q)$ , as expected for CDWs. Our findings also agree with earlier STS experiments of BSCCO [8–10], which found that the incommensurate checkerboard order has a dominant PDW character [68–71]. The proposed PDW scenario explains why the signal detected in X-ray scattering of cuprates is orders of magnitude smaller than the one observed in ordinary CDW materials ( $\delta n \ll \delta \Delta$ ).

Our method can be further extended to include the effects of magnetic fields by considering a Hubbard model with complex hopping elements (Peirls substitution). In type-II superconductors, external magnetic field generate isolated vortices in whose core the pairing gap is locally suppressed. Hence, a magnetic vortex acts as a pinning site for a PDW modulation, in analogy to the bond impurity considered in this Letter. Numerical studies of the Hubbard model in the presence of magnetic fields have indeed found that spatial modulations of the pairing gap develop in the proximity of the vortex core [72–74]. This finding is consistent with STS experiments demonstrating that the periodic modulations are mostly pronounced in the vicinity of the vortex core [7, 39, 75, 76], as well as with evidence that the density waves become long ranged at high magnetic fields [2, 3, 6, 22]. By locally suppressing superconductivity, large densities of magnetic vortices can lead to a long ranged PDW order.

We thank Peter Abbamonte, Lucio Braicovich, Debanjan Chowdhury, Riccardo Comin, J. C. Seamus Davis, Andrea Damascelli, Eugene Demler, Giacomo Ghiringhelli, Marco Grilli, Jenny Hoffman, Amit Keren, Steve Kivelson, and Dror Orgad for useful discussions. This work is supported by the Israel Science Foundation grant No. 151/19.

- 
- [1] J. Tranquada, B. Sternlieb, J. Axe, Y. Nakamura, and S. Uchida, *nature* **375**, 561 (1995).
  - [2] N. Doiron-Leyraud, C. Proust, D. LeBoeuf, J. Levallois,

- J.-B. Bonnemaïson, R. Liang, D. Bonn, W. Hardy, and L. Taillefer, *Nature* **447**, 565 (2007).
- [3] T. Wu, H. Mayaffre, S. Krämer, M. Horvatić, C. Berthier, W. Hardy, R. Liang, D. Bonn, and M.-H. Julien, *Nature* **477**, 191 (2011).
- [4] E. Fradkin and S. A. Kivelson, *Nature Physics* **8**, 864 (2012).
- [5] D. LeBoeuf, S. Krämer, W. Hardy, R. Liang, D. Bonn, and C. Proust, *Nature Physics* **9**, 79 (2013).
- [6] T. Wu, H. Mayaffre, S. Krämer, M. Horvatić, C. Berthier, P. L. Kuhns, A. P. Reyes, R. Liang, W. Hardy, D. Bonn, *et al.*, *Nature communications* **4**, 2113 (2013).
- [7] J. Hoffman, E. Hudson, K. Lang, V. Madhavan, H. Eisaki, S. Uchida, and J. Davis, *Science* **295**, 466 (2002).
- [8] C. Howald, H. Eisaki, N. Kaneko, M. Greven, and A. Kapitulnik, *Physical Review B* **67**, 014533 (2003).
- [9] M. Vershinin, S. Misra, S. Ono, Y. Abe, Y. Ando, and A. Yazdani, *Science* **303**, 1995 (2004).
- [10] T. Hanaguri, C. Lupien, Y. Kohsaka, D.-H. Lee, M. Azuma, M. Takano, H. Takagi, and J. Davis, *Nature* **430**, 1001 (2004).
- [11] G. Ghiringhelli, M. Le Tacon, M. Minola, S. Blanco-Canosa, C. Mazzoli, N. Brookes, G. De Luca, A. Frano, D. Hawthorn, F. He, *et al.*, *Science* **337**, 821 (2012).
- [12] J. Chang, E. Blackburn, A. Holmes, N. B. Christensen, J. Larsen, J. Mesot, R. Liang, D. Bonn, W. Hardy, A. Watenphul, *et al.*, *Nature Physics* **8**, 871 (2012).
- [13] D. H. Torchinsky, F. Mahmood, A. T. Bollinger, I. Božović, and N. Gedik, *Nature materials* **12**, 387 (2013).
- [14] E. Blackburn, J. Chang, M. Hücker, A. Holmes, N. B. Christensen, R. Liang, D. Bonn, W. Hardy, U. Rütt, O. Gutowski, *et al.*, *Physical review letters* **110**, 137004 (2013).
- [15] R. Comin, A. Frano, M. M. Yee, Y. Yoshida, H. Eisaki, E. Schierle, E. Weschke, R. Sutarto, F. He, A. Soumyanarayanan, *et al.*, *Science* **343**, 390 (2014).
- [16] E. H. da Silva Neto, P. Aynajian, A. Frano, R. Comin, E. Schierle, E. Weschke, A. Gyenis, J. Wen, J. Schneeloch, Z. Xu, *et al.*, *Science* **343**, 393 (2014).
- [17] M. Le Tacon, A. Bosak, S. Souliou, G. Dellea, T. Loew, R. Heid, K. Bohnen, G. Ghiringhelli, M. Krisch, and B. Keimer, *Nature Physics* **10**, 52 (2014).
- [18] M. Hashimoto, G. Ghiringhelli, W.-S. Lee, G. Dellea, A. Amorese, C. Mazzoli, K. Kummer, N. Brookes, B. Moritz, Y. Yoshida, *et al.*, *Physical Review B* **89**, 220511 (2014).
- [19] W. Tabis, Y. Li, M. Le Tacon, L. Braicovich, A. Kreyssig, M. Minola, G. Dellea, E. Weschke, M. Veit, M. Ramazanoglu, *et al.*, *Nature communications* **5**, 5875 (2014).
- [20] M. Huecker, N. B. Christensen, A. Holmes, E. Blackburn, E. M. Forgan, R. Liang, D. Bonn, W. Hardy, O. Gutowski, M. v. Zimmermann, *et al.*, *Physical Review B* **90**, 054514 (2014).
- [21] A. Achkar, X. Mao, C. McMahon, R. Sutarto, F. He, R. Liang, D. Bonn, W. Hardy, and D. Hawthorn, *Physical review letters* **113**, 107002 (2014).
- [22] S. Gerber, H. Jang, H. Nojiri, S. Matsuzawa, H. Yasumura, D. Bonn, R. Liang, W. Hardy, Z. Islam, A. Mehta, *et al.*, *Science* **350**, 949 (2015).
- [23] M. Hamidian, S. Edkins, K. Fujita, A. Kostin, A. Mackenzie, H. Eisaki, S. Uchida, M. Lawler, E.-A. Kim, S. Sachdev, *et al.*, arXiv preprint arXiv:1508.00620 (2015).
- [24] Y. Peng, M. Salluzzo, X. Sun, A. Ponti, D. Betto, A. Ferretti, F. Fumagalli, K. Kummer, M. Le Tacon, X. Zhou, *et al.*, *Physical Review B* **94**, 184511 (2016).
- [25] L. Chaix, G. Ghiringhelli, Y. Peng, M. Hashimoto, B. Moritz, K. Kummer, N. Brookes, Y. He, S. Chen, S. Ishida, *et al.*, *Nature Physics* **13**, 952 (2017).
- [26] Y. Peng, R. Fumagalli, Y. Ding, M. Minola, S. Caprara, D. Betto, M. Bluschke, G. De Luca, K. Kummer, E. Lefrançois, *et al.*, *Nature materials* **17**, 697 (2018).
- [27] H. Jang, S. Asano, M. Fujita, M. Hashimoto, D. Lu, C. Burns, C.-C. Kao, and J.-S. Lee, *Physical Review X* **7**, 041066 (2017).
- [28] M. Bluschke, M. Yaari, E. Schierle, G. Bazalitsky, J. Werner, E. Weschke, and A. Keren, arXiv preprint arXiv:1906.05021 (2019).
- [29] M. Kang, J. Pellicari, A. Frano, N. Breznay, E. Schierle, E. Weschke, R. Sutarto, F. He, P. Shafer, E. Arenholz, *et al.*, *Nature Physics* **15**, 335 (2019).
- [30] C. Castellani, C. Di Castro, and M. Grilli, *Physical review letters* **75**, 4650 (1995).
- [31] C. Castellani, C. Di Castro, and M. Grilli, *Physica C: Superconductivity* **282**, 260 (1997).
- [32] R.-H. He, M. Hashimoto, H. Karapetyan, J. Koralek, J. Hinton, J. Testaud, V. Nathan, Y. Yoshida, H. Yao, K. Tanaka, *et al.*, *Science* **331**, 1579 (2011).
- [33] H.-D. Chen, O. Vafek, A. Yazdani, and S.-C. Zhang, *Physical review letters* **93**, 187002 (2004).
- [34] P. A. Lee, *Physical Review X* **4**, 031017 (2014).
- [35] C. Pépin, V. De Carvalho, T. Kloss, and X. Montiel, *Physical Review B* **90**, 195207 (2014).
- [36] H. Freire, V. S. De Carvalho, and C. Pépin, *Physical Review B* **92**, 045132 (2015).
- [37] Y. Wang, D. F. Agterberg, and A. Chubukov, *Physical Review B* **91**, 115103 (2015).
- [38] Y. Wang, D. F. Agterberg, and A. Chubukov, *Physical review letters* **114**, 197001 (2015).
- [39] S. D. Edkins, A. Kostin, K. Fujita, A. P. Mackenzie, H. Eisaki, S. Uchida, S. Sachdev, M. J. Lawler, E.-A. Kim, J. S. Davis, *et al.*, *Science* **364**, 976 (2019).
- [40] M. Hamidian, S. Edkins, S. H. Joo, A. Kostin, H. Eisaki, S. Uchida, M. Lawler, E.-A. Kim, A. Mackenzie, K. Fujita, *et al.*, *Nature* **532**, 343 (2016).
- [41] D. F. Agterberg, J. Davis, S. D. Edkins, E. Fradkin, D. J. Van Harlingen, P. A. Lee, L. Radzihovsky, J. M. Tranquada, Y. Wang, *et al.*, arXiv preprint arXiv:1904.09687 (2019).
- [42] E. G. Dalla Torre, D. Benjamin, Y. He, D. Dentelski, and E. Demler, *Physical Review B* **93**, 205117 (2016).
- [43] R. Arpaia, S. Caprara, R. Fumagalli, G. De Vecchi, Y. Peng, E. Andersson, D. Betto, G. De Luca, N. Brookes, F. Lombardi, *et al.*, arXiv preprint arXiv:1809.04949 (2018).
- [44] S. Sachdev and R. La Placa, *Physical review letters* **111**, 027202 (2013).
- [45] K. Efetov, H. Meier, and C. Pépin, *Nature Physics* **9**, 442 (2013).
- [46] A. Allais, J. Bauer, and S. Sachdev, *Physical Review B* **90**, 155114 (2014).
- [47] Y. Caplan, G. Wachtel, and D. Orgad, *Physical Review B* **92**, 224504 (2015).
- [48] Y. Caplan and D. Orgad, *Physical review letters* **119**, 107002 (2017).

- [49] In contrast to Ref. [42, 77], we work here under the assumption that resonant *elastic* X-ray scattering is analogous to hard X-ray scattering and can be simply modeled as a density response. This approach is justified by the observation that measurements of YBCO using the two techniques lead to similar results [11, 12].
- [50] A. Altland and B. D. Simons, *Condensed matter field theory* (Cambridge university press, 2010).
- [51] According to the interpretation of the pseudogap as a precursor of the superconducting pairing gap [78], this approach applies to the pseudogap region as well.
- [52] S. Massidda, N. Hamada, J. Yu, and A. Freeman, *Physica C: Superconductivity* **157**, 571 (1989).
- [53] Increasing the hole doping reduces the antinodal distance and, accordingly, reduces the CDW/PDW wavevector observed in BSCCO [15, 79] and YBCO [14, 20]. Some authors [15, 27] disputed this interpretation due to the mismatch between the wavevector observed in X-ray experiments and the antinodal distance observed in ARPES. We point out that this mismatch is rather small (of the order of 10%) and is of the same order as the mismatch between the antinodal distances obtained by fitting the ARPES data with different phenomenological band structures [15, 80]. Furthermore X-ray scattering is sensitive to the bulk of the material, while ARPES is a surface probe. Hence, the mismatch between these two probes may be due to the common bulk-surface dichotomy of the chemical potential.
- [54] Note that the integrals in Eq.3 involve diverging functions. To normalize these expressions, we computed analytically  $\chi(\mathbf{q}, \Omega = i\Gamma)$  and performed a sum over  $N = 151$  equally spaced points using  $\Gamma/t = 0.1$ . We checked that the qualitative features of the resulting plots do not depend on the normalization procedure.
- [55] M. Norman, M. Randeria, H. Ding, and J. Campuzano, *Physical Review B* **52**, 615 (1995).
- [56] R. Markiewicz, S. Sahrakorpi, M. Lindroos, H. Lin, and A. Bansil, *Physical Review B* **72**, 054519 (2005).
- [57] P. Fulde and R. A. Ferrell, *Physical Review* **135**, A550 (1964).
- [58] A. Larkin and Y. N. Ovchinnikov, *Soviet Physics-JETP* **20**, 762 (1965).
- [59] E. Berg, E. Fradkin, and S. A. Kivelson, *Physical Review B* **79**, 064515 (2009).
- [60] E. Berg, E. Fradkin, S. A. Kivelson, and J. M. Tranquada, *New Journal of Physics* **11**, 115004 (2009).
- [61] G. Ghiringelli, private communication (unpublished).
- [62] R. Micnas, J. Ranninger, and S. Robaszkiewicz, *Journal of Physics C: Solid State Physics* **21**, L145 (1988).
- [63] R. Micnas, J. Ranninger, and S. Robaszkiewicz, *Reviews of Modern Physics* **62**, 113 (1990).
- [64] P. Monthoux and D. Scalapino, *Physical review letters* **72**, 1874 (1994).
- [65] D. Newns, C. Tsuei, and P. Pattanaik, *Physical Review B* **52**, 13611 (1995).
- [66] T. Husslein, I. Morgenstern, D. Newns, P. Pattanaik, J. Singer, and H. Matuttis, *Physical Review B* **54**, 16179 (1996).
- [67] The relative standard deviation of  $X$  is defined as  $\delta X \equiv (\sum_j X_j^2)^{1/2} / \sum_j X_j$ .
- [68] T. Pereg-Barnea and M. Franz, *Physical Review B* **68**, 180506 (2003).
- [69] E. Nowadnick, B. Moritz, and T. Devereaux, *Physical Review B* **86**, 134509 (2012).
- [70] E. G. Dalla Torre, Y. He, D. Benjamin, and E. Demler, *New Journal of Physics* **17**, 022001 (2015).
- [71] Z. Dai, Y.-H. Zhang, T. Senthil, and P. A. Lee, *Physical Review B* **97**, 174511 (2018).
- [72] J.-X. Zhu, I. Martin, and A. Bishop, *Physical review letters* **89**, 067003 (2002).
- [73] M. Takigawa, M. Ichioka, and K. Machida, *Journal of the Physical Society of Japan* **73**, 450 (2004).
- [74] S. Simonucci, P. Pieri, and G. Strinati, *Physical Review B* **87**, 214507 (2013).
- [75] K. Matsuba, S. Yoshizawa, Y. Mochizuki, T. Mochiku, K. Hirata, and N. Nishida, *Journal of the Physical Society of Japan* **76**, 063704 (2007).
- [76] S. Yoshizawa, T. Koseki, K. Matsuba, T. Mochiku, K. Hirata, and N. Nishida, *Journal of the Physical Society of Japan* **82**, 083706 (2013).
- [77] P. Abbamonte, E. Demler, J. S. Davis, and J.-C. Campuzano, *Physica C: Superconductivity* **481**, 15 (2012).
- [78] V. Emery and S. Kivelson, *Nature* **374**, 434 (1995).
- [79] W. Wise, M. Boyer, K. Chatterjee, T. Kondo, T. Takeuchi, H. Ikuta, Y. Wang, and E. Hudson, *Nature Physics* **4**, 696 (2008).
- [80] J. D. King, J. Rosen, W. Meevasana, A. Tamai, E. Rozbicki, R. Comin, G. Levy, D. Fournier, Y. Yoshida, H. Eisaki, *et al.*, *Physical review letters* **106**, 127005 (2011).